

Mn(V)(O) versus Cr(V)(O) Porphyrinoid Complexes: Structural Characterization and Implications for Basicity Controlling H-Atom Abstraction

Regina A. Baglia, Katharine A. Prokop-Prigge, Heather M. Neu, Maxime A. Siegler, and David P. Goldberg*

Department of Chemistry, The Johns Hopkins University, 3400 North Charles Street, Baltimore, Maryland 21218, United States

S Supporting Information

ABSTRACT: Isomorphous crystals of Mn^V(O) and Cr^V(O) corrolazines were characterized by single crystal X-ray diffraction. Reactivity studies with H atom donors and separated PCET reagents show a dramatic difference in H atom abstracting abilities for these two complexes. The implied large difference in driving force is opposite the trend in redox potentials, indicating that basicity is a key factor in determining the striking difference in reactivity for two metal-oxo species in identical ligand environments.

The ability of high-valent metal-oxo complexes to abstract hydrogen atoms from organic compounds is of critical importance to the functioning of metal-based oxidation catalysts. Included among these catalysts are enzymatic systems that utilize both heme and nonheme metal active sites.^{1,2} How the metal ion, the coordinating ligands, and surrounding protein matrix in the case of biological catalysts control the reactivity of metal-oxo intermediates in H atom abstraction is a question of fundamental importance. In heme enzymes, the Cytochrome P450s are among the most powerful H atom abstractors, utilizing compound I ((Fe^{IV}(O)(porph^{•+}))(cys)) for strong C–H cleavage.¹ The large driving force presented for H atom abstraction by P450 can be related to the bond dissociation free energy (BDFE) of the O–H bond of compound II (Fe^{IV}(OH)(porph)(cys)), formed after H atom transfer (HAT). The O–H BDFE can be further dissected into electron (E°) and proton (pK_a) affinities (or basicity), and evidence indicates that it is the elevated basicity of the Fe^{IV}=O unit in Cpd-II ($pK_a \approx 12$) that provides an advantage in driving force for HAT.^{1c,e}

Attempts to synthesize biomimetic high-valent metal-oxo species and to examine their propensity for HAT has led to parallel insights regarding the thermodynamic control of these reactions.^{3,4} These studies have helped support the analysis of the biological systems and supplied information for the design of synthetic oxidation catalysts. However, much remains to be learned regarding how the metal ion and ligand(s) of M(O)(L_n) complexes tune M(O–H) BDFEs, redox potentials, pK_a s, and ultimately HAT reactivity.

In this communication we compare the H atom abstraction abilities of Mn^V(O) and Cr^V(O) porphyrinoid complexes. Both of these complexes are characterized by single crystal X-ray diffraction (XRD). To our knowledge, the manganese complex is

the first example of a structurally characterized Mn^V(O) complex in a heme-type environment. The Cr and Mn complexes are isomorphous, providing a unique opportunity to determine the inherent HAT reactivity of Mn^V(O) versus Cr^V(O) moieties. Although Cr^V(O) complexes, including porphyrins, are known, little information is available regarding their H atom abstraction abilities.⁵ In this communication we show that Cr^V(O) is a better 1-e⁻ oxidant than Mn^V(O), but is a much weaker H atom abstractor.

The synthesis of Mn^V(O)(TBP₈Cz) (TBP₈Cz = octakis(*p*-*tert*-butylphenyl)corrolazinato³⁻) was carried out in a manner similar to that previously reported.^{4a} Addition of freshly prepared PhIO (10 equiv) to Mn^{III}(TBP₈Cz) (1) in CH₂Cl₂ gives the oxidized Mn^V(O)(TBP₈Cz) (2), which can be purified by silica gel chromatography. Dissolution of 2 in toluene to give a dark green solution followed by slow vapor diffusion of CH₃CN leads to the growth of dark green needles after a few days. These crystals were suitable for X-ray structure determination, and the structure of 2 is shown in Figure 1. Previous attempts at growing crystals of 2 in other solvent combinations were plagued by decomposition of the complex. However, we observed that 2 was stable in toluene/CH₃CN for at least 2 weeks and favored slow crystal growth. This crystallization method was also highly reproducible. As depicted in Figure 1, the Mn^V ion is 5-

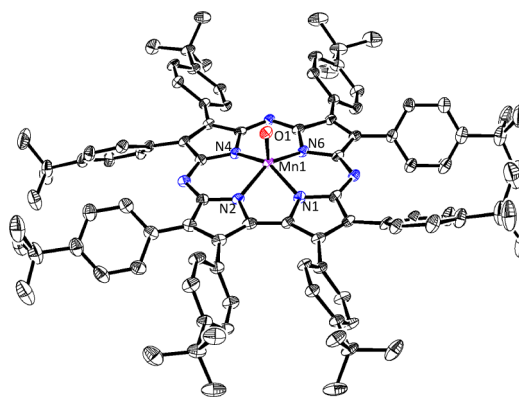


Figure 1. Displacement ellipsoid plot (50% probability level) of Mn^V(O)(TBP₈Cz) (2) at 110(2) K. H atoms and disorder are omitted for clarity.

Received: May 18, 2015

Published: August 21, 2015

coordinate, with Mn–N_{pyrrole} distances between 1.873(2)–1.8974(19) Å, and a short Mn–O distance of 1.5455(18) Å consistent with an Mn≡O triple bond. These distances are in agreement with those determined previously by EXAFS ($d(\text{Mn–O}) = 1.56$ Å, $d(\text{Mn–N}_{\text{pyrrole}}) = 1.88$ Å).^{4a} Structurally characterized nonheme complexes have Mn–O bond distances of 1.548(4)–1.558(4) Å, which are comparable with that of **2**.⁶ The manganese ion in **2** is significantly displaced by ca. 0.59 Å from the plane of the four pyrrole N atoms toward the terminal oxo ligand. For the isoelectronic Mn^V(NMe_s)(TBP₈Cz), the terminal mesitylimido Mn–N distance is slightly longer at 1.595(4)–1.611(4) Å, while the Mn ion is less displaced out of the N_{pyrrole} plane (Mn–N₄(plane) = 0.55 Å).^{4c} The structure unequivocally shows that the Mn^V(O) complex is 5-coordinate, as opposed to the proposed structures for related Mn^V(O) porphyrins.⁷

The analogous Cr^V(O)(TBP₈Cz) (**3**) was synthesized by aerobic, oxidative metalation of the metal-free corrolazine, TBP₈CzH₃, with Cr(CO)₆ in refluxing toluene.^{5d} No significant color change from the deep green of the metal-free starting material ($\lambda_{\text{max}} = 456, 679$ nm) was noted, but monitoring the reaction by UV–vis revealed distinct shifts in both the Soret and Q-band regions (**3**: $\lambda_{\text{max}} = 448, 653$ nm). Complex **3** was purified by flash chromatography (eluent: 60:40, CH₂Cl₂/hexanes) and recrystallized from vapor diffusion of acetonitrile into a toluene solution of **3** over 1 week. An X-ray structure determination was carried out and the structure of **3**, which is isomorphous with the Mn^V(O) complex, is shown in Figure S1. The Cr^V ion is 5-coordinate as seen for Mn, and $d(\text{Cr–O}) = 1.553(2)$ Å. This distance is similar to that seen for Cr^V(O) corroles (~1.57 Å).^{5d,8} The out of plane displacement of the chromium in **3** (Cr–N₄(plane) = 0.61 Å) is slightly larger than that seen for the corrole analogues (0.56–0.58), probably arising from the smaller cavity size of corrolazine (*trans*-N_{pyrrole}–N_{pyrrole}: 3.61 Å) versus corrole (*trans*-N_{pyrrole}–N_{pyrrole}: 3.67–3.69 Å). The metal-oxo distance for **3** is identical to that of **2**, but the M–N_{pyrrole} distances are slightly longer for **3** versus **2** (see Table S1). The out-of-plane distance for **3** is also slightly larger than **2**. These observations are consistent with the larger ionic radius of the Cr^V versus Mn^V ion.⁹

The EPR spectrum (9.44 GHz, 294 K) of **3** is shown in Figure S3. A nine line signal centered at $g = 1.987$ is observed, consistent with a Cr^V (d^1 , $S = 1/2$) ion with hyperfine coupling to four equivalent pyrrole nitrogen atoms (¹⁴N, $I = 1$). The satellite signals at high and low fields are due to hyperfine splitting from ⁵³Cr (9.5% abundant, $I = 3/2$). Evans method NMR measurement gave a magnetic moment of $\mu_{\text{eff}} = 1.36 \mu_{\text{B}}$, which is close to the predicted spin-only value of $1.73 \mu_{\text{B}}$ for an $S = 1/2$ ion. These data confirm the +5 oxidation state of the Cr ion and rule out the involvement of other potential ground state electronic configurations, such as Cr^{IV}(O)(TBP₈Cz^{•+}).^{4g,h}

Prior to examining the reactivity of the Cr^V(O) complex **3**, we synthesized the reduced chromium(III) analogue to obtain a spectroscopic benchmark for this species. Addition of triphenylphosphine, an oxygen atom acceptor, to **3** in toluene, followed by slow vapor diffusion of CH₃CN over the course of 2 weeks led to X-ray quality crystals of Cr^{III}(TBP₈Cz)(CH₃CN)₂ (**4**). The crystal structure of **4** is shown in Figure S5. Complex **4** is 6-coordinate, with the Cr^{III} ion bound by two axial CH₃CN molecules. Unlike in **3**, the Cr ion is displaced from the N₄(plane) by only 0.013 Å to accommodate the sixth ligand. The UV–vis spectrum of **4** in CH₂Cl₂ gives Soret and Q-bands at 465 and 709 nm, respectively, which are easily distinguished from those observed for the Cr^V(O) complex. The low-temperature

EPR spectrum of **4** (9.44 GHz, 12 K) is consistent with the $S = 3/2$ ground state expected for the Cr^{III} (d^3) ion (Figure S7).^{8a}

The Mn^V(O) and Cr^V(O) complexes are ideal candidates for examining the relative reactivity of high-valent, biomimetic metal-oxo complexes bound in identical ligand environments. Previously, we showed that **2** reacts with a range of H atom donors, including both substituted phenols (O–H bonds) and hydrocarbon (C–H) substrates, which exhibited bond dissociation energies (BDEs) from 66–80 kcal/mol.^{4b,d} We examined complex **3** for its potential reactivity toward substrates with similar bond strengths. A rapid reaction between **3** and excess TEMPOH in CH₂Cl₂ was observed by UV–vis spectroscopy, resulting in the isosbestic conversion of **3** (448, 653 nm) to a Cr^{III} product with a spectrum similar to **4** in the presence of excess TEMPOH (Figure 2a, Figure S10). The corresponding yield of

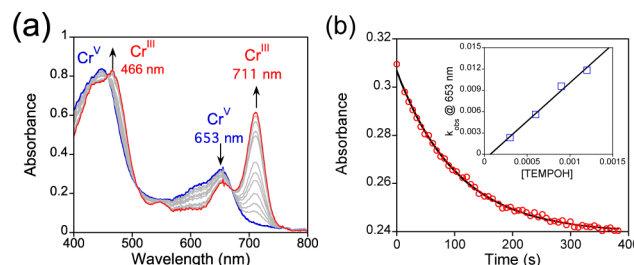
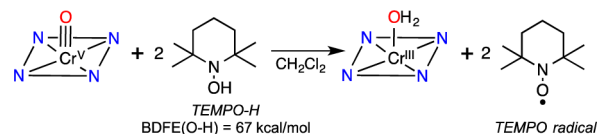


Figure 2. (a) UV–vis spectral changes (0–3 min) for the reaction of **3** (12 μM) with TEMPOH (150 equiv) at 25 °C. (b) Change in absorbance at 653 nm versus time corresponding to the decay of **3** (red circles) and best fit (black line). Inset: second-order rate plot.

TEMPO[•] was 82% (EPR quantitation) or 1.62 equiv relative to **3**. These data indicate the stoichiometry for this reaction follows that shown in Scheme 1, in which two equiv of TEMPOH react

Scheme 1



with **3** to give one equiv of reduced Cr^{III} product and two equiv of TEMPO[•] product. No Cr^{IV} intermediates were observed. This reaction exhibited pseudo-first-order behavior over 5 half-lives, and a plot of k_{obs} (s^{-1}) values correlated linearly with [TEMPOH] to give a second-order rate constant of $k_2 = 16 \pm 1 \text{ M}^{-1} \text{ s}^{-1}$ (Figure 2b). A kinetic isotope effect of $k_{\text{H}}/k_{\text{D}} = 5.2 \pm 0.6$ was measured for TEMPOH/D (Figure S9). These observations are consistent with a concerted H atom transfer (HAT) mechanism for the reaction of **2** with TEMPOH.

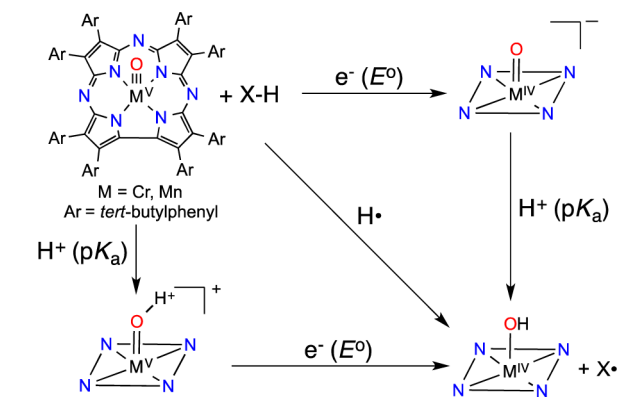
As seen in Table 1, complex **3** was only capable of oxidizing TEMPOH, with a weak O–H bond of 67 kcal/mol. It was unreactive toward other H atom donors, even under higher temperatures and prolonged reaction times. For example, a mixture of **3** and excess xanthene (BDFE = 73.3 kcal/mol) in toluene at 70 °C for 40 h gives back only starting material. In contrast, the Mn^V(O) complex **2** reacts with substrates that have BDFEs up to 80 kcal/mol.

A thermodynamic analysis of H atom abstraction for **2** and **3** can provide insight into the differences in reactivity seen for these two complexes. H atom abstraction by the metal-oxo complexes can be described as shown in Scheme 2, where HAT follows

Table 1. Reaction of 2 (Mn^V(O)) or 3 (Cr^V(O)) with H-Atom Donors (C–H and O–H) with a Range of BDFEs

substrate	Mn ^V (O)	Cr ^V (O)	BDFE ^{3a}
HMB ^a	no	no	83
2,4,6-TTBP ^b	yes	no	80
DHA ^c	yes	no	77
xanthene	yes	no	73
TEMPOH	yes	yes	67

^aHMB = hexamethylbenzene. ^b2,4,6-TTBP = 2,4,6-tri-*tert*-butylphenol. ^cDHA = 9,10-dihydroanthracene.

Scheme 2

either the concerted (diagonal) or stepwise electron-transfer (ET, horizontal) and proton-transfer (PT, vertical) steps shown in the square scheme. The thermodynamic parameters (E° , pK_a) associated with the ET and PT steps combined with the free energy of formation of the hydrogen atom (C_G), can be used to calculate the bond dissociation free energy (BDFE) for M(O–H), eq 1.^{10a} The difference in BDFE (Δ BDFE) for Mn^{IV}(OH) versus Cr^{IV}(OH) is expressed in eq 2 and relies only on the differences in E° and pK_a , eliminating the requirement for an accurate measure of C_G . Assuming the reaction is under thermodynamic control, the BDFE of the M(O–H) bond must be similar to or greater than the X–H bond being cleaved in the substrate. The correlation of HAT reactivity with BDFE has been observed for metal-oxo complexes.³ The results in Table 1 indicate that the BDFE for Mn^{IV}(OH) should be between 80–83 kcal/mol, whereas for Cr^{IV}(OH) the BDFE is 67–73 kcal/mol. These data imply a Δ BDFE of at least 8 kcal/mol for these two complexes.¹¹

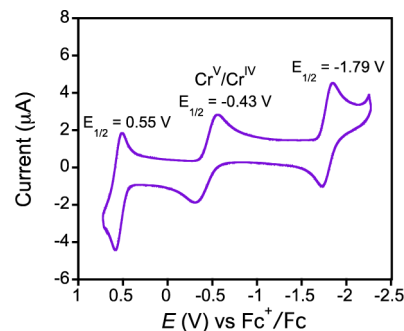
$$\text{BDFE}(\text{kcal/mol}) = 1.37pK_a + 23.06E^\circ + C_G \quad (1)$$

$$\Delta\text{BDFE} = 1.37\Delta pK_a + 23.06\Delta E^\circ \quad (2)$$

The Mn^V(O) and Cr^V(O) complexes were also capable of reacting with separated electron-transfer/proton-transfer reagents through a proton-coupled electron-transfer (PCET) mechanism. It has been shown that an effective “BDFE” for separate reductant/acid pairs can be calculated from their individual E° and pK_a values.^{10b,c} Complex 2 reacts with the reductant dimethylferrocene (Me₂Fc) ($E_{1/2} = -0.24$ V versus Fc⁺/Fc in CH₃CN) in the presence of the H⁺ donor acetic acid ($pK_a = 23.5$), to give Mn^{III}(TBP₃Cz)(OH₂) in CH₂Cl₂ as shown by UV–vis (Figure S13). However, no reaction occurs with either Me₂Fc or CH₃CO₂H alone, supporting a PCET process.^{4e} The BDFE for the Me₂Fc/CH₃CO₂H pair is 81.6 kcal/mol in CH₃CN ($C_G = 54.9$ kcal/mol). However, replacement of the

Me₂Fc reductant with unsubstituted Fc ($E_{1/2} = 0.00$ V) leads to no reaction. An effective BDFE = 87.1 kcal/mol is calculated for Fc/CH₃CO₂H. Similar experiments with the Cr^V(O) complex showed efficient PCET from Me₂Fc and trifluoroacetic acid (TFA) ($pK_a = 12.6$) to give Cr^{III}(TBP₃Cz), but no reaction was observed for Fc/TFA. These reductant/acid pairs have effective BDFEs of 66.5 and 75.5 kcal/mol, respectively. The results obtained for the separated PCET reagents provide good support for the BDFE range predicted for both 2 and 3 from the reactivity pattern with the H atom donors in Table 1.

Insight into the origin of the large difference in BDFE and related reactivity for 2 and 3 comes from cyclic voltammetry (Figure 3). The quasi-reversible wave at $E_{1/2} = -0.43$ V is

**Figure 3.** CV of 3 in CH₂Cl₂ with 0.1 M TBAPF₆ as supporting electrolyte; scan rate 25 mV/s.

assigned to the Cr^V/Cr^{IV} redox potential based on previous assignments for metallocorrolazines, including 2.^{4a} Interestingly, the Cr^V/Cr^{IV} potential is ~100 mV more positive than that seen for Mn^V/Mn^{IV} ($E_{1/2}(2) = -0.55$ V). According to eq 1, the larger redox potential for 3 should provide a 2.3 kcal/mol ($23.06 \times (0.1$ V)) increase in BDFE compared to 2. However, the BDFE for Cr^{IV}(OH) appears to be weaker than the BDFE for Mn^{IV}(OH) by at least 8 kcal/mol based on the observed HAT and PCET reactivity. Assuming a Δ BDFE of 8 kcal/mol, and including the measured $\Delta E^\circ = -0.1$ V, we find that ΔpK_a must be ~8 according to eq 2. This result indicates that a reduced [Mn^{IV}(O)⁻] species is at least 8 orders of magnitude more basic than the corresponding [Cr^{IV}(O)⁻], and this basicity dominates the difference in driving force for H atom abstraction. We previously suggested that the basicity of [Mn^{IV}(O)⁻] was a potential key factor in HAT,^{4b} and more recent studies have supported this conclusion.¹² However, this study provides a rare direct comparison of two high-valent metal-oxo species in identical ligand environments and demonstrates that a dramatic difference in reactivity can be assigned to the different basicities of the metal-oxo units.

In summary, we report a new Cr^V(O) porphyrinoid complex, and the first X-ray structure of an Mn^V(O) porphyrinoid complex. A comparison of HAT/PCET reactivity for these two adjacent first-row metal-oxo complexes (Mn, Cr) in identical ligand environments implies that the Mn^V(O) complex must have a much larger driving force (~8 kcal/mol) for H[•] abstraction than the corresponding Cr^V(O) complex, despite the latter complex having a 100 mV larger $E_{1/2}$ value. The larger driving force can be attributed to the basicity of the one-electron reduced [Mn^{IV}(O)⁻], which we estimate to be ~8 orders of magnitude more basic than [Cr^{IV}(O)⁻]. This work supports the hypothesis that the basicity of high-valent metal-oxo species in heme enzymes is a critical factor in tuning reactivity.

■ ASSOCIATED CONTENT

■ Supporting Information

The Supporting Information is available free of charge on the ACS Publications website at DOI: 10.1021/jacs.5b05142.

$\text{Cr}^{\text{III}}(\text{TBP}_8\text{Cz})(\text{CH}_3\text{CN})_2$ (CIF)

$\text{Cr}^{\text{V}}(\text{O})(\text{TBP}_8\text{Cz})$ (CIF)

$\text{Mn}^{\text{V}}(\text{O})(\text{TBP}_8\text{Cz})$ (CIF)

Experimental procedures, kinetic studies, EPR, CV, Figures S1–S14, and Table S1 (PDF)

■ AUTHOR INFORMATION

Corresponding Author

*dpg@jhu.edu

Notes

The authors declare no competing financial interest.

■ ACKNOWLEDGMENTS

We thank the NIH (GM101153 to D.P.G.) for financial support. R.A.B. is grateful for the E²SHI, George E. Owen, and Harry and Cleio Greer Fellowships.

■ REFERENCES

- (1) (a) Denisov, I. G.; Makris, T. M.; Sligar, S. G.; Schlichting, I. *Chem. Rev.* **2005**, *105*, 2253. (b) Rittle, J.; Green, M. T. *Science* **2010**, *330*, 933. (c) Yosca, T. H.; Rittle, J.; Krest, C. M.; Onderko, E. L.; Silakov, A.; Calixto, J. C.; Behan, R. K.; Green, M. T. *Science* **2013**, *342*, 825. (d) Poulos, T. L. *Chem. Rev.* **2014**, *114*, 3919. (e) Yosca, T. H.; Behan, R. K.; Krest, C. M.; Onderko, E. L.; Langston, M. C.; Green, M. T. *J. Am. Chem. Soc.* **2014**, *136*, 9124.
- (2) (a) Krebs, C.; Galonić Fujimori, D.; Walsh, C. T.; Bollinger, J. M. *Acc. Chem. Res.* **2007**, *40*, 484. (b) Bruijninx, P. C.; van Koten, G.; Gebbink, R. J. K. *Chem. Soc. Rev.* **2008**, *37*, 2716.
- (3) (a) Warren, J. J.; Tronic, T. A.; Mayer, J. M. *Chem. Rev.* **2010**, *110*, 6961. (b) Borovik, A. S. *Chem. Soc. Rev.* **2011**, *40*, 1870. (c) Bigi, J. P.; Harman, W. H.; Lassalle-Kaiser, B.; Robles, D. M.; Stich, T. A.; Yano, J.; Britt, R. D.; Chang, C. J. *J. Am. Chem. Soc.* **2012**, *134*, 1536. (d) Usharani, D.; Lacy, D. C.; Borovik, A. S.; Shaik, S. *J. Am. Chem. Soc.* **2013**, *135*, 17090. (e) Nam, W.; Lee, Y.-M.; Fukuzumi, S. *Acc. Chem. Res.* **2014**, *47*, 1146. (f) Chen, Z.; Yin, G. *Chem. Soc. Rev.* **2015**, *44*, 1083. (g) Puri, M.; Que, L., Jr. *Acc. Chem. Res.* **2015**, DOI: 10.1021/acs.accounts.5b00244.
- (4) (a) Lansky, D. E.; Mandimutsira, B.; Ramdhanie, B.; Clausén, M.; Penner-Hahn, J.; Zvyagin, S. A.; Telsler, J.; Krzystek, J.; Zhan, R.; Ou, Z.; Kadish, K. M.; Zakharov, L.; Rheingold, A. L.; Goldberg, D. P. *Inorg. Chem.* **2005**, *44*, 4485. (b) Lansky, D. E.; Goldberg, D. P. *Inorg. Chem.* **2006**, *45*, 5119. (c) Lansky, D. E.; Kosack, J. R.; Narducci Sarjeant, A. A.; Goldberg, D. P. *Inorg. Chem.* **2006**, *45*, 8477. (d) Prokop, K. A.; de Visser, S. P.; Goldberg, D. P. *Angew. Chem., Int. Ed.* **2010**, *49*, 5091. (e) Fukuzumi, S.; Kotani, H.; Prokop, K. A.; Goldberg, D. P. *J. Am. Chem. Soc.* **2011**, *133*, 1859. (f) Cho, K.; Leeladee, P.; McGown, A. J.; DeBeer, S.; Goldberg, D. P. *J. Am. Chem. Soc.* **2012**, *134*, 7392. (g) Leeladee, P.; Baglia, R. A.; Prokop, K. A.; Latifi, R.; de Visser, S. P.; Goldberg, D. P. *J. Am. Chem. Soc.* **2012**, *134*, 10397. (h) Baglia, R. A.; Dürr, M.; Ivanović-Burmazović, I.; Goldberg, D. P. *Inorg. Chem.* **2014**, *53*, 5893.
- (5) (a) Groves, J. T.; Haushalter, R. C. *J. Chem. Soc., Chem. Commun.* **1981**, 1165. (b) Garrison, J. M.; Bruice, T. C. *J. Am. Chem. Soc.* **1989**, *111*, 191. (c) Collins, T. J.; Slebodnick, C.; Uffelman, E. S. *Inorg. Chem.* **1990**, *29*, 3433. (d) Meier-Callahan, A. E.; Gray, H. B.; Gross, Z. *Inorg. Chem.* **2000**, *39*, 3605. (e) Bakac, A.; Guzei, I. A. *Inorg. Chem.* **2000**, *39*, 736. (f) Hess, J. S.; Leelasubcharoen, S.; Rheingold, A. L.; Doren, D. J.; Theopold, K. H. *J. Am. Chem. Soc.* **2002**, *124*, 2454. (g) O'Reilly, M.; Falkowski, J. M.; Ramachandran, V.; Pati, M.; Abboud, K. A.; Dalal, N. S.; Gray, T. G.; Veige, A. S. *Inorg. Chem.* **2009**, *48*, 10901. (h) Cho, J.; Woo, J.; Eun Han, J.; Kubo, M.; Ogura, T.; Nam, W. *Chem. Sci.* **2011**, *2*,

2057. (i) Kotani, H.; Kaida, S.; Ishizuka, T.; Sakaguchi, M.; Ogura, T.; Shiota, Y.; Yoshizawa, K.; Kojima, T. *Chem. Sci.* **2015**, *6*, 945.

(6) (a) Collins, T. J.; Gordon-Wylie, S. W. *J. Am. Chem. Soc.* **1989**, *111*, 4511. (b) MacDonnell, F. M.; Fackler, N. L. P.; Stern, C.; O'Halloran, T. V. *J. Am. Chem. Soc.* **1994**, *116*, 7431.

(7) (a) Groves, J. T.; Lee, J.; Marla, S. S. *J. Am. Chem. Soc.* **1997**, *119*, 6269. (b) Arunkumar, C.; Lee, Y.-M.; Lee, J. Y.; Fukuzumi, S.; Nam, W. *Chem. - Eur. J.* **2009**, *15*, 11482.

(8) (a) Meier-Callahan, A. E.; Di Bilio, A. J.; Simkhovich, L.; Mahammed, A.; Goldberg, I.; Gray, H. B.; Gross, Z. *Inorg. Chem.* **2001**, *40*, 6788. (b) Egorova, O. A.; Tsay, O. G.; Khatua, S.; Huh, J. O.; Churchill, D. G. *Inorg. Chem.* **2009**, *48*, 4634. (c) Egorova, O. A.; Tsay, O. G.; Khatua, S.; Meka, B.; Maiti, N.; Kim, M.-K.; Kwon, S. J.; Huh, J. O.; Bucella, D.; Kang, S.-O.; Kwak, J.; Churchill, D. G. *Inorg. Chem.* **2010**, *49*, 502.

(9) Shannon, R. D. *Acta Crystallogr., Sect. A: Cryst. Phys., Diffr., Theor. Gen. Crystallogr.* **1976**, *32*, 751.

(10) (a) Bordwell, F. G.; Cheng, J. P.; Harrelson, J. A. *J. Am. Chem. Soc.* **1988**, *110*, 1229. (b) Waidmann, C. R.; Miller, A. J. M.; Ng, C.-W. A.; Scheuermann, M. L.; Porter, T. R.; Tronic, T. A.; Mayer, J. M. *Energy Environ. Sci.* **2012**, *5*, 7771. (c) Tarantino, K. T.; Liu, P.; Knowles, R. R. *J. Am. Chem. Soc.* **2013**, *135*, 10022.

(11) This ΔBDFE assumes that the BDFE of $\text{Cr}^{\text{IV}}(\text{OH})$ is below that of xanthene, i.e., 72 kcal/mol or less, whereas the BDFE of $\text{Mn}^{\text{IV}}(\text{OH})$ is assumed to be ≥ 80 kcal/mol.

(12) Green, M. T. *Curr. Opin. Chem. Biol.* **2009**, *13*, 84 and references therein.